Revision 3

Ilmenite-magnetite-spinel spheroids in a garnetite layer associated with eclogite and garnet peridotite, Blanský les Granulite Massif, Czech Republic, are melt droplets

Stanislav Vrána[1], Lukáš Ackerman[2,1], Vojtěch Erban[1] and Patricie Halodová[1]

[1] Czech Geological Survey, Klárov 3, 118 21 Praha 1, Czech Republic

[2] Institute of Geology, The Czech Academy of Sciences, Rozvojová 269, 165 00, Praha 6, Czech Republic.

Abstract

Interlayered eclogite and symplectitic garnet rock that is interpreted as former garnetite are found in the Gföhl Unit of the Bohemian Massif. They show unusual Fe–Ti-rich compositions, characterized by TiO_2 contents up to 2.34 wt. %, and Mg-numbers of 59.8 and 51.6, respectively. Equilibration conditions of 1250 °C and 4.0 GPa are calculated for eclogite. The petrogenesis of this rock association can be best explained as high-temperature and ultra-high-pressure magmatic cumulates. Highly decoupled Sr-Nd isotopic composition with nearly constant radiogenic $^{87}Sr/^{86}Sr$ values and a slightly negative ε Nd value suggests interaction of aqueous fluid most likely derived from a subducting slab and/or from parental magmas. The garnetite contains large (up to 0.5 mm) Fe–Ti-rich spheroids of ilmenite–magnetite–spinel, interpreted as frozen droplets of a melt incorporated in the growing garnet. The interstices between these garnet crystals are filled by ilmenite–magnetite–spinel

This is a preprint, the final version is subject to change, of the American Mineralogist (MSA)
Cite as Authors (Year) Title. American Mineralogist, in press.
(DOI will not work until issue is live.) DOI: http://dx.doi.org/10.2138/am-2016-5298

aggregates, with concave outer surfaces with trapped Fe–Ti-rich melt. These ilmenite-magnetite-spinel spheroids represent possibly the first record of such an oxidized assemblage in mantle rocks, and probably the first description of Fe–Ti-rich melt in eclogite–garnetite mantle rocks. A calculation based on mineral proportions in the spheroids and mineral composition indicates that the immiscible Fe–Ti-rich melt consisted of 29.8 TiO_2, 5.1 Al_2O_3, 0.2 Cr_2O_3, 24.5 Fe_2O_3, 37.4 FeO, 0.9 MnO, and 2.1 MgO wt%. Petrology and geochemistry of the garnetite indicates an unusual composition for an upper mantle melt with a high oxygen fugacity and relatively high Fe content.

Keywords: ilmenite–magnetite–spinel, Fe–Ti-rich melt, UHP crystallization, garnetite, eclogite, garnet peridotite, Moldanubian Zone

Introduction

Eclogite and garnet pyroxenite represent a volumetrically minor, but very important rock types, inasmuch as they provide direct evidence for heterogeneity in the upper mantle. Their petrogenesis is a matter of debate. They have been variously interpreted as basaltic protoliths recycled back to the upper mantle (e.g., Allègre and Turcotte 1986) and/or high-pressure crystal cumulates derived from migrating transient basaltic melts (e.g., Becker 1996; Medaris et al. 1995; Pearson et al. 1993). Eclogites show a wide range of major element, trace element and isotopic composition reflecting the heterogeneity of their protoliths and/or parental melts. Exceptionally Fe–Ti-rich eclogites are rather rare, and their petrogenesis is a matter of debate (e.g., Liu et al., 2007). In the Gföhl Unit of the Moldanubian Zone, Bohemian Massif, garnet peridotites, associated eclogites and garnet pyroxenites are widespread (Medaris et al. 1995a;

Always consult and cite the final, published document. See http://www.minsocam.org or GeoscienceWorld

Medaris et al. 1995b; Medaris et al. 2005; Medaris et al., 2006; Faryad 2009; Medaris et al. 2013; Faryad et al. 2013). The peridotites usually form variably serpentinized decimeter- to kilometer-sized bodies enclosed in high temperature – high pressure crustal rocks such as granulite, gneiss, and/or migmatite. The crustal rocks occur as centimeter to decimeter sized lenses, layers and/or dikes within, or closely associated with, garnet peridotite.

Spheroid is a non-genetic term for a spheroidal or spherical particle. Spheroidal shape is obtained by rotating an ellipse about one of its principal axes (shape more or less similar to a sphere). Examples in the literature include tiny metallic spheroids at impact sites (e.g. Meteor Crater, Arizona), in some tektites and lunar regolith (Mead et al. 1965; Blau et al. 1973), ilmenite-magnetite aggregates in gabbro (Liu et al. 2014), pyrite aggregates formed in various environments (McClay and Ellis 1983), reduction spheroids in sediments (Hofmann 1991), and various applications in technology (Jacobs et al. 1976). Spheroid is not a common term in upper mantle petrology.

In this study, we report detailed petrography, major/trace element and Sr-Nd isotopic geochemistry for the Fe–Ti-rich eclogite–symplectitic garnet rock. We interpret the ilmenite–magnetite–spinel assemblage as having crystallized from an immiscible Fe–Ti melt under upper mantle conditions at relatively high oxygen fugacity. The spheroids of ilmenite–magnetite–spinel are interpreted as crystallized melt droplets trapped in growing garnet.

Geological setting and samples

The Bohemian Massif represents the easternmost and largest exposure of the Variscan orogenic belt in Europe, which formed during the Late Paleozoic collision of Gondwana, Laurasia and intervening microcontinents (Franke 1989; Matte 2001; Schulmann et al. 2009). The massif has been divided into four major tectonic zones: the Teplá–Barrandian, Saxothuringian, Moldanubian, and Moravo–Silesian. The Moldanubian Zone consists of three different units: the Monotonous, the Varied and the Gföhl, the latter showing the highest grade of metamorphism (2.3 GPa, 850–1050 °C; Vrána et al. 2013). In the Moldanubian Zone of southern Bohemia, large lenses of garnet and spinel peridotites are enclosed in predominantly felsic kyanite-garnet granulites of the Blanský les Granulite Massif (Kodym 1972, Medaris et al. 2005; Naemura et al. 2009; Franěk et al. 2011; Vrána et al. 2013). Based on their lithology, chemical composition and the P/T regime, Medaris et al. (2005, Table 1) characterized three types of peridotites (Types I, II and III) in the Gföhl Unit.Given the widespread overlaps in lithology and chemistry, Al_2O_3 content in orthopyroxene serves as a reliable distinguishing feature: Type I: 2.3–6.3 Al_2O_3 in Opx; Type II: 0.7–2.1 Al_2O_3 in Opx; Type III: 0.4–1.9 Al_2O_3 in Opx. Type I peridotites comprise both spinel- and garnet-bearing varieties, contain high-Al_2O_3 orthopyroxene, and equilibrated in a low P/T regime. Type II peridotites are characterized by generally lower Mg#'s than those of Type I, association with abundant pyroxenite, the local coexistence of garnet and spinel, low-Al_2O_3 orthopyroxene and a range of P/T regimes. Type III peridotites have the most uniform characteristics among the three groups, consisting solely of garnet peridotite (with one exception) with low- Al_2O_3 orthopyroxene and a medium P/T regime.

Garnet peridotite from Hamry, near the Chlum locality of the present study (Fig. 1), was characterized by Medaris et al (2005) as Type III, equilibrated at T=1245 °C and 4.43 GPa. Garnet pyroxenites and eclogites in the Czech Type II peridotites were interpreted as high-pressure crystal cumulates from melts that migrated through the lithospheric mantle (Medaris et al. 1995a; Becker 1996; Ackerman et al. 2009). It is particularly interesting that Nd, Sr and O isotope analyses and negative Eu anomalies in the Gföhl garnet pyroxenites indicate that subducted oceanic crust contributed to melts from which they crystallized (Medaris et al. 1995a; Ackerman et al. 2009).

The Chlum locality (48^{o}54’18” N, 14^{o}16’52” E) and Hamry locality (Medaris et al. 2005) are shown in Fig. 1. A twenty cm long fragment of an interlayered eclogite and symplectitic garnet rock was collected from a large Type III mafic/ultramafic lens 0.5 km west of the Chlum village (Fig. 1) as a loose piece. Fairly fresh loose pieces of garnet peridotite, kyanite-garnet felsic granulite and garnet-bearing two-pyroxene mafic granulite accompany the eclogite and symplectitic garnet rock (sample BD112 and BD110, respectively). Because it is likely that boudins of mantle rocks can be relatively small and somewhat variable, it is uncertain whether the garnet peridotite collected at the same place (sample BD134) has a direct relationship to the eclogite and symplectitic garnet sample or might be derived from another boudin.

Minor layers of eclogite and garnet pyroxenite within bodies of garnet peridotite are common throughout the Bohemian Massif (Medaris et al. 1995a,b, Medaris et al. 2006). What makes geological interpretation difficult is the polyphase deformation history of the hosting felsic granulites, including typically two to three deformation events, penetrative shearing and metamorphic reactions under granulite and amphibolite facies. These processes transformed peridotite bodies to elongated lenses, such as seen in Fig. 1. A similar lenticular/boudin shape is characteristic for mafic granulites (garnet-bearing two-pyroxene rocks) of dioritic to gabbroid composition down to meter-scale bodies scattered in felsic granulites. There is information indicating that many of these mafic boudins are retrogressed eclogites (Vrána et al. 2013), which were completely metamorphosed to two-pyroxene ± biotite rock without garnet during low-P, high-T decompression. Other mafic samples show incomplete decompression reactions involving omphacite and partial garnet breakdown dominantly to orthopyroxene and plagioclase.

Methods

Major-element whole-rock analysis was performed by wet chemical methods in the laboratory of the Czech Geological Survey, Prague. The relative 2σ uncertainties are smaller than 1 % (SiO_2), 2 % (FeO), 5 % (Al_2O_3, K_2O, Na_2O), 7 % (TiO_2, MnO, CaO), 6 % (MgO) and 10 % (Fe_2O_3, P_2O_5) (Dempírová 2010). Minor and trace elements in whole-rock samples were determined by the Thermo Element2 ICP-MS in the Institute of Geology, Academy of Sciences of the Czech Republic, with a precision better than 5 % for each element analyzed. The accuracy of the analyses was monitored by means of long-term reproducibility of BCR-2 reference material (USGS), yielding values between 5 and 15 % of recommended values (Jochum and Nohl 2008).

Major element mineral composition was obtained using a CAMECA SX 100 WDS electron microprobe in the Institute of Geological Sciences, Masaryk University, and Czech Geological Survey, Brno. The analytical conditions varied according to the mineral analyzed, but typically 15 kV accelerating voltage, beam current of 10–20 nA and acquisition time of 10-30 s were employed. The main standards used were spessartine (Si, Mn), almandine (Fe), andradite (Ca), $MgAl_2O_4$ (Mg), hornblende (Ti), sanidine (Al, K), albite (Na), fluorapatite (P) and chromite (Cr). Mineral abbreviations follow the convention of Whitney and Evans (2010).

Trace element concentrations in clinopyroxene and garnet were determined by laser ablation ICP-MS, using an Element2 mass spectrometer (Thermo), coupled with a 213-nm laser system (NewWave Research). The analytical conditions followed those of Ackerman et al. (2012). The analytical precision of all elements was always better than 5 %. The accuracy was monitored by the analysis of BCR-2G material yielding values better than 10 % for most analyzed elements in comparison to values of Jochum and Nohl (2008).

For the strontium and neodymium isotopic determinations, dissolved garnet and clinopyroxene mineral separates were isolated from the rest of the elements by column exchange chromatography using Eichrom Sr.spec, TRU.spec and Ln.spec resins (see Míková and Denková 2007, and references therein). Isotopic analysis was performed on a Finnigan MAT 262 thermal ionization mass spectrometer at the Czech Geological Survey in the dynamic mode, using a single Re filament with Ta activator solution for Sr and double Re filament assembly for Nd. The $^{143}Nd/^{144}Nd$ ratios were corrected for mass bias to $^{146}Nd/^{144}Nd = 0.7219$, $^{87}Sr/^{86}Sr$ ratios assuming $^{86}Sr/^{88}Sr = 0.1194$. External reproducibility was controlled by repeated analyses of the JNdi-1 with $^{143}Nd/^{144}Nd = 0.512107 \pm 17$ (1σ, n = 14) and NBS 987 with $^{87}Sr/^{86}Sr = 0.710232 \pm 10$ (1σ, n = 14) isotopic standards. The Rb, Sr, Sm and Nd concentrations for age determination were obtained using ICP-MS solution analyses as described above.

Modal analysis of symplectite in sample BD110 was conducted on Tescan MIRA 3GMU fitted with SDD X-Max^N 80mm^2 EDS detector and AZtecEnergy AutoPhaseMap software (Oxford Instruments) at the Czech Geological Survey. Three areas of interest, 500 µm by 500 µm, were chosen. For each area an EDS map was individually acquired, all at high magnification (405x), resolution of 1024x1024pixels, step size 500 nm, accelerating voltage of 7 kV, WD 15 mm, 365counts/pixel. These conditions enabled the precise phase identification and calculation of percentage of individual minerals. For image analysis of mineral proportions in ilmenite–magnetite–spinel spheroids or proportion of the same mineral aggregates in symplectite of the sample BD110, NIS Element program was used.

Results

Petrography

The composite sample of eclogite–symplectitic garnet rock consists of an eclogite layer with garnet completely preserved, and very fine-grained 4 cm layer in which garnet was extensively replaced by plagioclase-orthopyroxene-clinopyroxene-spinel symplectite (Figs. 2a,c). This layer contains relict garnet grains and opaque mineral aggregates amounting to c. 7.4 vol%.

The eclogite has a nearly isotropic fabric. The typical grain size of garnet (c. 54 vol%) and clinopyroxene (43 vol%) is 1–4 mm. The undeformed granoblastic structure and mineral compositions are largely preserved. Some of the garnet-clinopyroxene interfaces are decorated by a narrow zone of khaki-colored pargasite, which turns to a brown variety in rims around ilmenite. The rock is cut by widely spaced fractures accompanied by minor secondary amphibole and by a dense network of subparallel straight fractures across both garnet and clinopyroxene (Fig. 2b). The total content of pargasite is estimated at 2–3 vol% and ilmenite at ~1%.

The symplectitic garnet rock (sample BD110) has a nearly isotropic fabric, as indicated by relict garnet and interstitial ilmenite–magnetite–spinel aggregates (Figs. 2c, d). The relict garnet is surrounded by very fine-grained symplectite, which constitutes as much as 74 vol% of the rock. The relict garnet accounts for ~20 vol%. The opaque mineral aggregates (Ilm+Mt+Spl) comprise ~7 vol%, have concave shapes and fill the interstitial spaces between areas of symplectite. The average modal composition of symplectite (wt%) is as follows:

anorthite 30.8, orthopyroxene 35.4, clinopyroxene + minor amphibole 16.8, spinel 14.7, magnetite 2.3. Modal analyses of three areas and their colour-coded maps are included in *Supplementary File 1.* In addition, a detail of frozen reaction of garnet to polymineralic symplectite with colour-coded minerals is given in Figure 4, whereas Figure 5 shows a sketch of textures of partly symplectitized garnetite and interpreted garnetite prior to symplectitization.

Aggregates of opaque minerals also occur as small 300–700 μm inclusions in the symplectite (Figs. 3a, b). Presumably the spheroidal inclusions were originally enclosed in the garnet. Image analysis of 11 spheroids yields the following modal composition (vol%): 56.4 ilmenite, 36.8 magnetite and 6.8 spinel. Detailed microprobe investigations revealed presence of accessory apatite and minor barite probably of a late hydrothermal origin in sample BD110.

The garnet peridotite, sample BD134, is a partially serpentinized lherzolite that shows a porphyroclastic texture. Large garnet grains 3–7 mm are rimmed by kelyphite within a fine-grained, 0.1–1.0 mm, olivine + orthopyroxene + clinopyroxene matrix (Fig. 6). Antigorite veinlets penetrate olivine aggregates and amount to ~15 vol%.

Whole-rock major and trace element chemical composition

The eclogite BD112 has a composition similar to that of other eclogites within the Gföhl Unit (Table 1; Medaris et al. 1995b) except for its very low Mg# [100 * Mg/(Mg+Fe)] of 59.8, which is similar to the eclogite sample from the Nové Dvory locality (Southern Moravia; Medaris *et al.*, 1995a). Such a low Mg #, accompanied by Na_2O>0.75 wt%, Cr_2O_3 <0.15 wt%, and Ni<200 ppm (Table 1), fulfills compositional criteria for distinguishing this rock as an eclogite rather than pyroxenite (Medaris et al. 1995a). In contrast, the whole-rock chemistry of the symplectitic garnet rock (BD110) is similar to that of the garnet in the same rock with an addition of several percent of ilmenite and magnetite. Correction of the whole-rock analysis of symplectitic garnet rock BD110 for 5.3 wt% of Fe-Ti oxides results in a composition (Tab. 1) that is closely comparable to microprobe analysis of relict garnet in the same sample (Tab. 1).

Rare earth element (REE) and extended trace element patterns samples BD112 and BD110, normalized to primitive mantle (PM - McDonough and Sun 1995), are given in Fig. 7. The eclogite exhibits overall REE concentrations higher than PM and a slight depletion in light rare earth elements (LREE) in comparison to heavy rare earth elements (HREE) with La_N/Yb_N of 0.5, coupled with a small negative anomaly (Eu/Eu* = 0.9). Among the other trace elements, the eclogite is enriched in some large ion lithophile elements (LILE) and U–Th but shows Nb, Rb and Sr negative anomalies. The symplectitic garnet rock BD110 differs from the eclogite by showing a sinusoidal REE pattern with enrichments for La–Ce with respect to Pr–Nd. Both are enriched in HREE.

Sr-Nd isotopic compositions

Strontinum and Nd isotopic data for whole-rock samples and mineral separates from Chlum are given in Table 2. They yield a poorly defined isochron age of 328 ± 54 Ma due to high errors on the calculated $^{147}Sm/^{144}Nd$ ratios. The data are plotted in Fig. 8 with the initial isotopic ratios recalculated at 330 Ma. When compared to other eclogites from the Bohemian Massif (Fig. 8), the Chlum samples exhibit very different Sr-Nd compositions with highly radiogenic and variable initial $^{87}Sr/^{86}Sr$ values of 0.70825–0.71033 and the highest value in whole-rock sample of symplectitic garnet rock. In comparison, calculated ε Nd values have only a very limited range between –1.2 and +0.4. Such compositions form a horizontal array

Always consult and cite the final, published document. See http://www.minsocam.org or GeoscienceWorld

This is a preprint, the final version is subject to change, of the American Mineralogist (MSA)
Cite as Authors (Year) Title. American Mineralogist, in press.
(DOI will not work until issue is live.) DOI: http://dx.doi.org/10.2138/am-2016-5298

in Fig. 8, where most of the samples overlap with the composition of the Enriched Mantle 2 (EM 2) component.

Mineral chemistry

Clinopyroxene

Clinopyroxene from the eclogite has Mg# of 73.3–74.7 and contains a high percentage of components other than diopside: 10.4–12.3 mol% jadeite, 4.6–5.1 mol% aegirine, and 8.0–9.5 mol% Ca-tschermak component. With Na_2O contents between 2.10 and 2.42 wt%, this pyroxene plots close to the divide between compositional fields of diopside and omphacite, with a low jadeite component (Morimoto et al. 1988). Minor variation in composition across the grains is documented by core and rim analyses (Table 3). Although these rocks do not contain omphacite, and therefore are not eclogites sensu stricto, they are commonly referred to as eclogites in the literature on the Bohemian massif (Beard et al. 1992; Medaris et al. 1995b; Medaris et al. 2005).

The clinopyroxene exhibits a typical LREE-enriched, convex-upward REE pattern (Fig. 7) with La_N/Yb_N of ~17 and no Eu anomaly. The extended trace element pattern resembles similar characteristics as the whole rock, except LILE which are largely depleted in clinopyroxene.

Garnet

In the eclogite, cores of garnet contain 35.2 mol% pyrope, 29.7 mol% almandine and 30.2 mol% grossular components, whereas the rim contains 34.3 mol% pyrope, 35.0 mol% almandine and 27.3 mol % grossular (Table 3). The chromium content is very low, with values from 0.02 to 0.04 wt% Cr_2O_3. In comparison, relict garnet in garnetite exhibits a more

Always consult and cite the final, published document. See http://www.minsocam.org or GeoscienceWorld

Mg-rich composition with 39.7–40.8 mol% pyrope, 28.9–29.4 mol% almandine and 26.9–27.5 mol% grossular. Also, the chromium content is somewhat higher (0.09 wt. % Cr_2O_3).

The garnets from the eclogite and symplectitic garnet rock show similar trace element characteristics, being largely depleted in LREE with respect to HREE (Fig. 7), reflected by very low La_N/Yb_N ratios between 0.006 and 0.007. In the eclogite, the extended trace element pattern for garnet is similar to that of clinopyroxene in spite of its general more pronounced depletions. In contrast to the pronounced major element compositional zoning in eclogite, garnet trace elements exhibit very little core-to-rim variations. Nevertheless, the garnet cores contain higher contents of HREE, Y, Nb and Li than do the rims (Table 5). Symplectite planimetric mineral analyses in sample BD110, characterized in the petrography section, in combination with microprobe analyses of the symplectite minerals, give a composition closely comparable with the mineral chemistry of the relict garnet as follows from comparison of columns 2 and 4 in Table 1.

Ilmenite–magnetite–spinel spheroids

Calculation based on mineral proportions obtained by image analysis and mineral chemistry (Table 4) results in the following composition of the Fe-Ti-rich spheroids (wt%): 28.7 TiO_2, 3.7 Al_2O_3, 0.2 Cr_2O_3, 27.9 Fe_2O_3, 37.0 FeO, 0.8 MnO, and 1.7 MgO. Magnetite in spheroids and in intersticial aggregates is free of exsolution lamellae of ilmenite, common in crustal gabbros (Beckman et al. 2015). On the other hand, magnetite contains minute exsolution lamellae of spinel, visible at high magnification, with 4.14 wt% Al_2O_3, 1.14 wt% MgO and 0.52 Cr_2O_3 (Table 6), indicating high-T crystallization in Al-rich system. Ilmenite contains elevated Mg contents (1.79 wt% MgO).

Garnet peridotite

Mineral analyses of two pyroxenes, garnet, and olivine from peridotite BD134 are presented in Table 7. The peridotite may or may not have a genetic relationship with the eclogite – garnetite but it provides independent information for comparison with sample BD112/110. Olivine in sample BD134 contains 89.3 mol% forsterite. Porphyroclastic garnet (Table 7; Fig. 6) contains 70.8–73.0 mol% pyrope, 14.4–16.5 mol% almandine, 5.2–5.7 mol% grossular, 4.6–4.7 mol% uvarovite, and minor andradite and spessartine. Clinopyroxene is highly magnesian with 40.2–41.1 mol% enstatite, and 13.7–14.2 mol% jadeite. Orthopyroxene contains 86.1–86.3 mol% enstatite and 1.8 mol% Ca-tschermak molecule.

Geothermobarometry

The garnet and clinopyroxene cores from eclogite equilibrated at a temperature of 1256 °C (Powell 1985; Ai 1994; Ganguly et al. 1996; Krogh-Ravna 2000) assuming a pressure estimate of 4.0 GPa (i.e. the pressure obtained by Medaris et al. 1995a for Type III peridotites), while the garnet and clinopyroxene rims yield 1090 °C. A pressure calculation for garnet peridotite BD134 was obtained using the Al-in-orthopyroxene barometer (Brey and Köhler 1990), assuming equilibrium temperature calculated from olivine-garnet and clinopyroxene-garnet pairs (T = 1100 °C; Harley 1984; Powell 1985; Ai 1994). This calculation yields a pressure of 3.41 GPa for the garnet peridotite, significantly lower than the 4.0 pressure calculated by Medaris et al. (1995a). However, using the higher temperature of T=1250 ºC obtained from eclogite BD112, the peridotite yields a pressure estimate of 4.23 GPa. This value for the Chlum peridotite agrees well with that for the nearby Hamry garnet peridotite (T=1245 ºC, P=4.43 GPa) by Medaris et al. (2005).

Always consult and cite the final, published document. See http://www.minsocam.org or GeoscienceWorld

Discussion

Petrogenesis of eclogite and symplectitic garnet rock

Whole-rock analysis of the symplectitic garnet rock, sample BD110 (Table 1), is similar to the composition of relict garnet in the same sample. If the analysis of the symplectitic garnet rock is corrected for the content of 5.3 wt% ilmenite+magnetite+spinel aggregates, as in column 3, Table 1, the resulting composition corresponds to the mineral chemistry of relict garnet in the same sample. As a following step, planimetric analysis of the mineralogical composition of symplectite was undertaken. Combination of this data with the chemistry obtained from microprobe analysis of symplectite minerals yielded a calculated composition of symplectite, shown in column 2, Table 1. Thus two independent methods show that the symplectitic garnet rock, sample BD110, was originally a garnetite, modified by extensive conversion of garnet to anorthite+orthopyroxene+clinopyroxene+spinel+magnetite symplectite in the process of low-P high-T decompression. Figure 5 shows a sketch of textures of partly symplectitized garnetite and the interpreted garnetite prior to symplectitization.

Widespread eclogites and garnet pyroxenites occurring within the Gföhl Unit of the Moldanubian Zone are usually interpreted as having been formed as high-pressure cumulates from transient, upper mantle-derived, basaltic melts with a significant contribution of recycled crustal material (Medaris et al. 1995a; Medaris et al. 2006; Ackerman et al. 2009; Medaris et al. 2013). Eclogite and garnetite described here differ significantly from previously studied rocks in several important ways: (1) very low Mg #, (2) very high TiO_2 contents (up to 2.34 wt. %), (3) almost flat whole-rock REE distribution above the primitive mantle values, (4) no significant Eu anomaly, (5) large scale Sr-Nd isotopic decoupling, and (6) high equilibration

Always consult and cite the final, published document. See http://www.minsocam.org or GeoscienceWorld

temperature (1256 °C for the eclogite). A similar Fe–Ti-rich eclogite with a low Mg # of 51.8–58.7 and TiO_2 contents up to 1.91 wt. % was described from the Úhrov locality in eastern Bohemia (Medaris et al. 1995); however, no magnetite or ilmenite–magnetite–spinel spheroids were reported from the Úhrov occurrence. The presence of eclogite and garnetite layers together in a single hand specimen strongly supports the idea of their formation by high-pressure crystal accumulation. If this is correct, the highly Fe–Ti-rich nature of the eclogite–garnetite association requires a specific parental magma which could reflect either a low degree of partial melting of mantle sources or extensive basaltic melt fractionation of olivine, clinopyroxene, and garnet. Highly decoupled Sr-Nd isotopic data forming a horizontal array, with initial radiogenic $^{87}Sr/^{86}Sr$ values of up to 0.71033 and a slightly negative ε Nd value (–1.2) in garnetite argue for a ^{87}Sr-rich fluid interaction, most likely derived from a subducting slab and/or derivation of parental magmas from subduction-related mantle overprinted by a hydrous fluid. No matter which process is correct, a high activity of H_2O is confirmed by the occurrence of minor amphibole within eclogite and garnetite. However, most of increased H_2O activity relates to a late decompression recrystallization stage; possibly, ^{87}Sr-rich fluid interaction took place during this late stage. Because the REE budget in eclogite is predominantly controlled by clinopyroxene and garnet, the REE composition of the melt from which eclogite crystallized can be directly calculated using the mineral composition of clinopyroxene and partitioning coefficients of Johnson (1998). This approach was discussed by Medaris et al. (2013) and it should be reliable, if the cumulate rock (eclogite) has a composition consistent with high temperature and $D_{cpx/grt}$ values that closely follow those obtained from high temperature experiments. Both requirements are met in the case of our eclogite sample. Thus, the calculated melt composition in equilibrium with clinopyroxene shows a highly enriched LREE composition with La_N/Yb_N ratio of ~207. Such a composition suggests a derivation of the parental melts from an enriched source with a significant contribution of continental material.

Ilmenite–magnetite–spinel spheroids and interstitial aggregates

Spheroids, originally enclosed in growing garnet crystals, are interpreted as former droplets of a Fe–Ti-saturated melt. Most of the Fe–Ti-rich melt filled the interstitial spaces between the settled garnet crystals (Fig. 2c). The trapped melt crystallized to form polymineralic aggregates. This textural information strongly supports a relatively early separation of immiscible Fe–Ti-rich melt from a silicate melt. Basaltic melts generally have a high Ti solubility (up to 9 wt. %; Green and Pearson 1986; Ryerson and Watson 1987) and, therefore, it is unlikely that they can reach Ti saturation. On the other hand, high CO_2 content in silicate melts can strongly reduce Ti solubility and hence permit magmas to reach their Ti saturation. Such alkaline magmas would have very low SiO_2, but high LREE contents, both features that are characteristic of the Chlum eclogite-garnetite association.

A recent study of magnetite-ilmenite (± hornblende ± phlogopite ± apatite) spheroids in cumulus olivine and interstitial aggregates in the mafic-ultramafic Baima intrusion in SW China (Liu et al. 2014) represents a strong case in support of relatively early separation of immiscible Fe-Ti-O melt. This intrusion is of Permian age and crystallized at mid-crustal to upper-crustal conditions. In the Chlum garnetite BD110, the melt crystallization took place under upper-mantle conditions at P=4.2 GPa and T=1240 °C. It is uncertain, what effect these high P–T conditions have on the process Fe–Ti-rich melt unmixing. To gain some information on the conditions of liquidus crystallization of ilmenite, magnetite and spinel, Fe-Ti oxides thermo-oxybarometry data could be applied. However, the low ulvöspinel component in magnetite (9.1 mol%, Table 5) indicates that the magnetite–ilmenite assemblage has been severely re-equilibrated during prolonged annealing (Hammond and Taylor 1982).

There is a puzzling difference in garnet preservation in BD112 eclogite compared to that in partly symplectitic BD110 garnetite, even though the garnet composition in both rocks is very similar. In garnetite, the formation of the Pl+Opx+Cpx+Spl decompression symplectite after garnet proceeded in a similar manner as it is common in local mafic and intermediate granulites (Owen and Dostal 1996; Vrána et al. 2013). In eclogite, there is minor pargasitic amphibole locally forming rims at the garnet interface with clinopyroxene, but no symplectite after garnet is present. We suggest that the nearly monomineralic garnetite was more affected by brittle deformation than was the pyroxene-bearing eclogite. If so, fractures allowed better access of fluids into garnetite, which promoted symplectite formation.

Implications

In a wider context, several types of liquid immiscibility in basaltic magmas are known at present. These include sulfide-rich melts in some layered intrusions (Pye et al. 1984), ilmenite and apatite-rich domains (nelsonites) in some gabbro-anorthosite massifs (Kolker 1982), microscopic scale silica-rich and Fe-rich inclusions documented from the Skaergaard intrusion (Jakobsen et al. 2005), and silicate domains in accumulations of native iron in trap formation in Siberia (Kamenetsky et al. 2013). The early separation of immiscible Fe–Ti-rich melt from crystallizing ferrobasaltic magma under shallow crustal conditions (Baima pluton, China), has been now recognized (Liu et al. 2014). The formation of Ilm+Mt+Spl spheroids in garnetite/eclogite association from Chlum, the Variscan belt in the Bohemian Massif, seems to be a single example of separation of immiscible Fe–Ti-rich melt under high PT conditions at present. We interpret these spheroids as crystallized from melt droplets. This may indicate probable occurrence of the Fe–Ti-rich melt unmixing across a range of pressure conditions.

The evidence for recycled crustal material within the upper mantle is indicated by Sr-Nd isotope composition of garnet pyroxenites and eclogites (Medaris et al. 1995; Brueckner and Medaris; Becker 1996; Ackerman et al. 2009), and gross chemical features of resulting eclogites and garnet pyroxenites. Liou and Tsujimori (2013) and Gilotti (2013) reviewed the ever-increasing abundance of mineral data on ultrahigh-pressure metamorphism involving subducted continental crust. The Chlum sample shows a potential of other, as yet unknown, compositional characteristics of the subducted crustal material. The novel information from Chlum garnetite–eclogite is the significant Fe–Ti-enrichment, demonstrated by high ilmenite and magnetite contents, and an elevated oxygen fugacity indicated by magnetite. The presence of ilmenite–magnetite–spinel spheroids in the Chlum garnetite sample sheds new light on redox variation in rocks with a history of mantle residence, but with a crustal/supracrustal component.

Acknowledgments

We would like to gratefully acknowledge the contribution of J. Gilotti, and the reviewers R.N. Abbott and H. Brueckner for their detailed and constructive reviews, which contributed to an improved version of the article. We thank P. Gadas, Faculty of Science, Masaryk University, Brno, for microprobe analyses and J. Ďurišová for ICP-MS analyses. M. Rieder critically read an early version of the manuscript. The study was supported by a Project of the Czech Geological Survey, No. 390000. This work was partly supported by the Scientific Programme

CEZ: RVO67985831 of the Institute of Geology, Academy of Sciences of the Czech Republic.

References cited

Ackerman, L., Jelínek, E., Medaris, G., Ježek, J., Siebel, W., and Strnad, L. (2009) Geochemistry of Fe-rich peridotites and associated pyroxenites from Horní Bory, Bohemian Massif: Insights into subduction-related melt–rock reactions. Chemical Geology, 250, 152–167.

Ackerman, L., Špaček, P., Medaris, L.G., Hegner, E., Svojtka, M., and Ulrych, J. (2012) Geochemistry and petrology of pyroxenite xenoliths from Cenozoic alkaline basalts, Bohemian Massif. Journal of Geosciences, 58,199–219.

Ai, Y. (1994) A revision of the garnet-clinopyroxene Fe^{2+}-Mg exchange geothermometer. Contributions to Mineralogy and Petrology, 115, 467–473.

Allégre, C.J. and Turcotte, D.L. (1986) Implications of a two component marble cake mantle. Nature, 323, 123–127.

Beard, B.L., Medaris, Jr.L.G., Johnson, C.M., Brueckner, H.K., Mísař, Z. (1992) Petrogenesis of Variscan high-temperature group A eclogites from the Moldanubian Massif, Czechoslovakia. Contribution to mineralogy and Petrology, 111, 468–483.

Beckman, V., Möller, C., Söderlund, U., Corfu, F., Pallon, J., and Chamberlain, K.R. et al. (2015) Metamorphic zircon formation at the transition from gabbro to eclogite in Trollheimen–Surnadalen, Norwegian Caledonides. Corfu, F., Gasser, D. & Chew, D. M. (eds) 2014. New Perspectives on the Caledonides of Scandinavia and Related Areas. Geological Society, London, Special Publications, 390, 403–424).

Becker, H. (1996) Crustal trace element and isotopic signatures in garnet pyroxenites from garnet peridotite massifs from lower Austria. Journal of Petrology, 37, 785–810.

Blau, P.J., Axon, H.J., and Goldstein, J.I. (1973) Investigation of the Canyon Diablo metallic spheroids and their relationship to the breakup of the Canyon Diablo meteorite. Journal of Geophysical Research 78, 363–374.

Brey, G.P. and Köhler, T. (1990) Geothermobarometry in four-phase lherzolites II. New thermobarometers, and practical assessment of existing thermobarometers. Journal of Petrology, 31, 1353–1378.

Dempírová, L. (2010) The evaluation of precision and relative error of the main components of silicate analyses in Central Laboratory of the CGS. Zprávy o geologických výzkumech v roce 2009. 326–330 (in Czech).

Faryad, S.W. (2009) The Kutná Hora Complex (Moldanubian zone, Bohemian Massif): A composite of crustal and mantle rocks subducted to HP/UHP conditions. Lithos, 109:193–208

Faryad, S.W., Jedlička, R. and Collett, S. (2013) Eclogite facies rocks of the Monotonous unit, clue to Variscan suture in the Moldanubian Zone (Bohemian Massif). Lithos, 179:353–363

Franěk, J., Schulmann, K., Lexa, O., Ulrich, S., Štípská, P., Haloda, J. and Týcová, P. (2011) Origin of felsic granulite microstructure by heterogeneous decomposition of alkali feldspar and extreme weakening of orogenic lower crust during the Variscan orogeny. Journal of Metamorphic Geology, 29, 103–130.

Franke, W. (1989) Tectonostratigraphic units in the Variscan belt of Central Europe. Geological Society of America, Special Paper 23, 67–90.

Ganguly, J., Cheng, W., and Tirone, M. (1996) Thermodynamics of alumosilicate garnet solid solution: new experimental data, an optimized model, and thermodynamic application. Contributions to Mineralogy and Petrology, 126, 137–151.

Gilotti, J.A. (2013) The realm of ultrahigh-pressure metamorphism. Elements, 9, 255–260.

Green, T. H. and Pearson, N. (1986) Ti-rich accessory phase saturation in hydrous mafic—felsic compositions at high P, T. Chemical Geology, 54, 185–201.

Hammond, P.A. and Taylor, L.A. (1982) The ilmenite/titanomagnetite assemblage: kinetics of reequilibration. Earth and Planetary Science Letters, 61, 143–150.

Harley, S.L. (1984) An experimental study of the partitioning of Fe and Mg between garnet and orthopyroxene. Contributions to Mineralogy and Petrology, 86, 359–373.

Hart, S. R. (1988) Heterogeneous mantle domains: signatures, genesis and mixing chronologies. Earth and Planetary Science Letters, 90, 273–296.

Hofmann, B.A. (1991) Mineralogy and geochemistry of reduction spheroids in Red Beds. Mineralogy and Petrology, 44, 107–124.

Jacobs, M.H., Law, T.J., Melford, D.A., and Stowell, M.J. (1976) Identification of heterogenous nuclei for graphite spheroids in chill-cast iron. Material Science and Technology, 3, 99–108.

Jakobsen, J.K., Veksler, I.V., Tegner, C., and Brooks, C.K. (2005) Immiscible iron- and silica-rich melts in basalt petrogenesis documented in the Skaergaard intrusion. Geology, 33, 885–888.

Jochum, K.P. and Nohl, U. (2008) Reference materials in geochemistry and environmental research and the GeoReM database. Chemical Geology 253:50–53

Johnson, K.T.M. (1998) Experimental determination of partition coefficients for rare earth and high-field-strength elements between clinopyroxene, garnet, and basaltic melt at high pressures. Contributions to Mineralogy and Petrology, 133, 60–68.

Kamenetsky, V.S., Charlier, B., Zhitova, L., Sharygin, V., Davidson, P. and Feig, S. (2013) Magma chamber–scale liquid immiscibility in the Siberian Traps represented by melt pools in native iron. Geology, 41, 1091–1094.

Kodym O. (1965) Geological map 1:25 000 of the Křemže area, 32-214. Geological Survey of the Czech Republic, Prague.

Kodym, O. (1972) Multiphase deformation in the Blanský les granulite massif (South Bohemia). Krystalinikum, 9, 91–105.

Kodym, O., Jakeš, P., and Schovánek, P. (1978) Granulite und ultramafische Gesteine aus der Strukturbohrung Holubov. Journal of Geological Sciences, Geology, 32, 7–47.

Kolker, A. (1982) Mineralogy and geochemistry of Fe–Ti oxide and apatite (nelsonite) deposits and evaluation of the liquid immiscibility hypothesis. Economic Geology, 77, 1146–1158.

Krogh Ravna, E. (2000) The garnet-clinopyroxene Fe^{2+}-Mg geothermometer: an updated calibration. Journal of Metamorphic Petrology, 18, 211–219.

Liou, J.G. and Tsujimori, T. (2013) The fate of subducted continental crust: evidence from recycled UHP–UHT minerals. Elements, 9, 248–250.

Liu, Y., Yang, H., Shau, Y., Meng, F., Zhang, J., Yang, J. and Yu, S. (2007) Compositions of high Fe–Ti eclogites from the Sulu UHP metamorphic terrane, China: HFSE decoupling and protolith characteristics. Chemical Geology, 239, 64–82.

Liu, P.P., Zhou, M.F., Chen, W.T., Boone, M. and Cnudde, V. (2014) Using multiphase solid inclusions to constrain the origin of the Baima Fe–Ti–(V) oxide deposits, SW China. Journal of Petrology, 55, 951–976.

Matte, P. (2001) The Variscan collage and orogeny (480-290 Ma) and the tectonic definition of the Armorica microplate: A review. Terra Nova, 13, 122–128.

McClay, K.R. and Ellis, P.G. (1983) Deformation and recrystallization of pyrite. Mineralogical Magazine, 47, 527–538.

McDonough, W. and Sun, S. (1995) The composition of the Earth. Chemical Geology, 120, 223–253.

Mead, C.A., Chao, E.C.T., and Littler, J. (1965) Metallic spheroids from Meteor Crater, Arizona. American Mineralogist 50, 667–681.

Medaris, G.Jr., Beard, B.L., Johnson, C.M., Valley, J.W. Spicuzza, M.J., Jelínek, E. and Mísař, Z. (1995a) Garnet pyroxenite and eclogite in the Bohemian Massif: geochemical evidence for Variscan recycling of subducted lithosphere. Geologische Rundschau, 84, 489–505.

Medaris, G.Jr., Jelínek, E. and Mísař, Z. (1995b) Czech eclogites: terrane settings and implications for Variscan tectonic evolution of the Bohemian Massif. European Journal of Mineralogy, 7, 7–28.

Medaris, G.Jr., Wang, H., Jelínek, E., Mihaljevič, M. and Jakeš, P. (2005) Characteristics and origins of diverse Variscan peridotites in the Gföhl Nappe, Bohemian Massif, Czech Republic. Lithos, 82, 1–23.

Medaris, L. G., Beard, B. L., and Jelínek, E. (2006) Mantle-Derived, UHP Garnet Pyroxenite and Eclogite in the Moldanubian Gföhl Nappe, Bohemian Massif: A Geochemical Review, New P-T Determinations, and Tectonic Interpretation. International Geology Review, 48, 765–777.

Medaris, G.L.Jr., Jelínek, E., Beard, B.L., Valley, J.W. Spicuzza, M.J., and Strnad, L. (2013) Garnet pyroxenite in the Biskupice peridotite, Bohemian Massif: anatomy of a Variscan high-pressure cumulate. Journal of Geosciences, 58, 3–19.

Míková, J. and Denková, P. (2007) Modified chromatographic separation scheme for Sr and Nd isotope analysis in geological silicate samples. Journal of Geosciences, 52, 221–226.

Morimoto, N., Fabries, J., Ferguson, A.K., Ginzburg, I.V., Ross, M., Seifert, F.A, Zussman, J., Aoki, K. and Gottardi, G. (1988) Nomenclature of pyroxenes. American Mineralogist, 73, 1123–1133.

Naemura, K., Hirajima, T. and Svojtka, M. (2009) The Pressure-Temperature Path and the Origin of Phlogopite in Spinel-Garnet Peridotites from the Blansky Les Massif of the Moldanubian Zone, Czech Republic. Journal of Petrology, 50, 1795–1827.

Owen, J.V., and Dostal, J. (1996) Contrasting corona structures in mafic granulite from the Blanský Les Complex, Bohemian Massif, Czech Republic. Canadian Mineralogist, 34, 959–966.

Pearson, D., Davies, G., and Nixon, P. (1993) Geochemical constraints on the petrogenesis of diamond facies pyroxenites from the Beni Bousera peridotite massif, North Morocco. Journal of Petrology, 34, 125–172.

Powell, R. (1985) Regression diagnostics and robust regression in geothermometer/geobarometer calibration: the garnet–clinopyroxene geothermometer revisited. Journal of Metamorphic Geology, 3, 231–243.

Always consult and cite the final, published document. See http://www.minsocam.org or GeoscienceWorld

This is a preprint, the final version is subject to change, of the American Mineralogist (MSA)
Cite as Authors (Year) Title. American Mineralogist, in press.
(DOI will not work until issue is live.) DOI: http://dx.doi.org/10.2138/am-2016-5298

Pye, E.G., Naldrett, A.J. and Giblin, P.E. (1984) The Geology and Ore Deposits of the Sudbury Structure. Ontario Geological Survey, Special Volume 1, Ontario Ministry of Natural Resources.

Ryerson, F. J. and Watson, E. B. (1987) Rutile saturation in magmas: implications for Ti—Nb—Ta depletion in island-arc basalts. Earth and Planetary Science Letters, 86, 225–239.

Schulmann, K., Konopásek, J., Janoušek, V., Lexa, O., Lardeaux, J-M., Edel, J., Štípská, P. and Ulrich, S. (2009) An Andean type Palaeozoic convergence in the Bohemian Massif. Comptes Rendus Geosci 341:266–286

Vrána, S., Janoušek, V. and Franěk, J. (2013). Contrasting mafic to felsic HP–HT granulites of the Blanský les Massif (Moldanubian Zone of southern Bohemia): complexity of mineral assemblages and metamorphic reactions. Journal of Geosciences, 58, 347–378.

Whitney, D.L. and Evans, B.W. (2010): Abbreviations for names of rock-forming minerals. American Mineralogist, 95, 185–187.

Figure captions

Figure 1. Simplified geology of the Křemže area in the central-eastern part of the Blanský les Granulite Massif. Adopted from 1:25 000 geological map (Kodym 1965).

Figure 2. (a) A section of eclogite (top) and symplectitic garnet rock (nearly black) layers, **(b)** garnet and clinopyroxene with minor pargasite and ilmenite in eclogite layer; scanner image in transmitted light,**(c)** garnetite with wide symplectite rims (black) around relict garnet, intersticial ilmenite–magnetite–spinelaggregates have concave outlines; small ilmenite–magnetite–spinel spheroids are framed yellow; macrophoto of polished slab, **(d)** symplectitic garnet rock with intersticial ilmenite–magnetite–spinel aggregates. Residual garnet exhibits a system of parallel fractures. At right bottom are two spheroids of Fe-Ti-oxides. Grt garnet; Sy symplectite; scanner image in transmitted light.

Always consult and cite the final, published document. See http://www.minsocam.org or GeoscienceWorld

Figure 3. (a) thin section of symplectitic garnet rock showing two Ilm + Mt + Spl spheroids in symplectite after garnet. Relict garnet (Grt) is preserved at top right, **(b)** ilmenite, magnetite and spinel I spheroid within symplectitic garnet rock; Magnetite contains two sets of minute spinel II lamellae.

Figure 4. A datail of frozen in reaction of garnet to polymineralic symplectite with colour-coded minerals. Sample BD110.

Figure 5. (a) Schematic diagram showing the textural and mineralogical changes in extensive decompression symplectitization of the garnetite, (b) the interpreted original texture of garnetite.

Figure 6. Garnet peridotite (BD134) with kelyphite reaction rims around garnet.

Figure 7. Rare earth element (REE) and extended trace element patterns of the studied eclogite, garnetite and their mineral phases normalized to primitive upper mantle values of McDonough and Sun (1995).

Figure 8. Initial (330 Ma) Sr-Nd isotopic compositions of whole-rock samples and mineral separates from Chlum eclogite and garnetite. Mantle components (DMM, EM1, EM2, HIMU) are from Hart (1988), calculated at 330 Ma. Composition of other Bohemian Massif eclogites from Medaris et al. (2006) and references therein are also plotted.

Table 1. Whole-rock major and trace element compositions of the studied eclogite and symplectitic garnet rock

Sample	BD112	BD110	BD110	BD110**	BD110		BD112	BD110	BD110
Rock/Mineral	eclogite	symplectitic garnet rock	composition calculated from symplectite modal analyses	whole-rock minus 5.3 wt% Ilm+Mt+Spl	relict garnet microprobe analysis**		Eclogite	symplectitic garnet rock	Garnet*
SiO_2 (wt%)	42.71	35.83	39.84	38.95	40.61	Y	40	76	85
TiO_2	1.21	2.34	0.22	0.89	0.22	Zr	79	91	58
Al_2O_3	16.09	20.06	22.23	21.58	22.04	Nb	2.2	6.1	0.01
Fe_2O_3	1.89	7.13			n.a.	Cs	0.61	1.2	n.a.
FeO	10.66	11.44	14.17	15.84	15.19	Ba	55.5	468	<0.02
MnO	0.27	0.44	0.39	0.43	0.5	La	3.9	4.3	0.036
MgO	10.34	10.68	12.40	11.50	10.92	Ce	12	6.7	0.35
CaO	14.85	9.4	10.30	10.81	10.86	Pr	2.1	0.77	0.18
Na_2O	1.05	0.08	0.04		b.d.	Nd	12	4.5	2.6
K_2O	0.05	0.04			b.d.	Sm	4.4	3.3	3.5
P_2O_5	0.04	0.05			0.02	Eu	1.4	1.4	1.6
CO_2	0.08	0.02			n.a.	Gd	5.9	7.4	7.8
H_2O+	0.77	1.02			n.a.	Tb	1.0	1.7	1.8
H_2O-	0.18	0.37			n.a.	Dy	7.1	13	13.6
Total	100.25	99.54	99.59	100.00	100.36	Ho	1.6	2.8	3.2
Mg #	59.8	51.6			56.2	Er	4.9	8.6	9.7
Li (ppm)	9.3	7.9			0.83	Tm	0.75	1.3	1.4
Sc	61	76			n.a.	Yb	4.9	8.7	10.2
V	379	380			n.a.	Lu	0.79	1.4	1.5
Cr	373	589			n.a.	Hf	2.4	2.01	1.0
Co	54	61			n.a.	Ta	0.36	0.76	<0.001
Ni	119	91			n.a.	W	0.49	1.1	n.a.
Cu	15	26			n.a.	Pb	3.4	3.0	0.09
Zn	71	51			n.a.	Bi	0.08	0.07	n.a.
Ga	15	10			n.a.	Th	1.8	3.8	0.08
Rb	0.82	1.6			<0.02	U	0.89	1.6	0.22
Sr	64	34			0.18				

BD110** - garnetite minus 5.3 wt% Ilm+Mt+Spl (see text for explanation)

** total includes 0.07 wt% Cr_2O_3. For the precision and accuracy of the analyses, see Methods section

Table 2. Sr-Nd isotopic composition of bulk rock samples BD110 and BD112 and rock-forming minerals of BD112

Sample	BD110	BD112	BD112	BD112	BD112
Fraction	Bulk Rock	Bulk Rock	Garnet	Clinopyroxene	Clinopyroxene + Pargasite
Rb (ppm)	1.57	0.82	0.38	6.53	4.97
Sr (ppm)	33.96	63.53	21.00	174.38	198.33
$^{87}Rb/^{86}Sr$	0.134	0.0374	0.0524	0.108	0.0725
$^{87}Sr/^{86}Sr$	0.710981	0.708814	0.709339	0.708421	0.708607
2S(M)	0.000015	0.000014	0.000013	0.000017	0.000011
$^{87}Sr/^{86}Sr$ (330 Ma)	0.71035	0.70864	0.70909	0.70791	0.70827
Nd (ppm)	4.53	12.24	6.53	19.30	19.44
Sm (ppm)	3.28	4.42	4.16	4.44	4.83
$^{147}Sm/^{144}Nd$	0.44	0.22	0.39	0.14	0.15
2S	0.06	0.03	0.06	0.02	0.02
$^{143}Nd/^{144}Nd$	0.513118	0.512705	0.513065	0.512507	□.512548
2S(M)	0.000020	0.000020	0.000015	0.000019	0.000021
$^{143}Nd/^{144}Nd$ (330 Ma)	0.512172	0.512233	0.512233	0.512207	0.512223
ε_{Nd} (330 Ma)	-0.8	0.4	0.4	-0.1	0.2

Measured $^{87}Sr/^{86}Sr$ and $^{143}Nd/^{144}Nd$ ratios with instrumental error expresed as double standard error of the mean (2S(M)). Rb, Sr, Sm and Nd concentrations determined using ICP-MS, $^{87}Rb/^{86}Sr$ and $^{147}Sm/^{144}Nd$ calculated

Table 3. Composition of minerals in garnet clinopyroxenite BD112

	garnet			clinopyroxene			ilmenite
sample	BD112	BD112		BD112	BD112		BD112
analysis	13 c	12 r		10 c	11 r		1
SiO_2	40.21	39.93		51.22	50.10		0
TiO_2	0.40	0.21		0.83	1.00		49.94
Al_2O_3	21.28	21.96		7.62	9.26		0
Cr_2O_3	0.04	0.02		0.00	0.00		0
FeO	16.37	17.88		7.10	6.25		45.37
MnO	0.43	0.49		0.00	0.08		0.34
MgO	9.25	9.16		11.76	11.30		2.06
CaO	12.52	11.01		19.79	20.28		0
Na_2O	0.01	0.01		2.36	2.11		0
total	100.51	100.67		100.68	100.38		97.71
oxygen No.	12	12		6	6		3
Si	3.007	2.992		1.873	1.833		
Al^{IV}	0.000	0.008		0.127	0.167		
Al^{VI}	1.882	1.935		0.201	0.232		
Ti	0.022	0.012		0.023	0.028		0.953
Cr	0.002	0.001		0.000	0.000		0.000
Fe^{3+}	0.076	0.046		0.048	0.029		0.095
Fe^{2+}	0.947	1.074		0.169	0.162		0.867
Mn	0.027	0.031		0.000	0.002		0.007
Mg	1.031	1.023		0.641	0.616		0.078
Ca	1.003	0.884		0.775	0.795		
Na				0.167	0.150		
total	7.999	8.007		4.024	4.015		
Mg#	50.2	47.7		74.7	73.3		
almandine	29.68	34.96	acmite	4.8	2.9	ilm	86.7
andradite	3.91	2.32	jadeite	11.9	12.1	geik	7.8
grossular	30.19	27.28	Ca-Ts	8.2	11.2	pyroph	0.7
pyrope	35.17	34.33	enstatite	32.0	30.8	hem	4.7
spessartine	0.93	1.04	orthoferrosilite	8.4	8.1		
uvarovite	0.12	0.06	wollastonite	33.5	32.8		

Standard deviations 2σ (wt%) are as follows: 0.20, 0.19 Si (Grt, Cpx), 0.13, 0.12 Al (Grt, Cpx), 0.31, 0.34 Fe (Grt, Cpx), 0.05, 0.09 Mg (Grt, Cpx), 0.19, 0.22 Ca (Grt, Cpx).

Table 4. Composition of minerals in symplectitic garnet rock BD110

				Fe - Ti - O spheroid			
	garnet			Ilm		Mt	Spl
sample	BD110	BD110		BD110		BD110	BD110
analysis	22	23		17		16	15
SiO_2	40.74	40.61				0.19	
TiO_2	0.18	0.22		51.17		3.43	0.05
Al_2O_3	22.38	22.04				4.14	60.26
Cr_2O_3	0.09	0.09		0.04		0.52	0.49
FeO	15.41	15.19		44.48		82.88	29.64
MnO	0.51	0.50		1.48		0.27	0.35
MgO	10.79	10.92		1.79		1.14	11.11
CaO	11.28	10.86				0.02	
Na_2O	0.02						
total	101.40	100.43		98.96		92.59	101.9
oxygen No.	12	12		3		4	4
Si	2.996	3.009					
Al^{IV}	0.004	0.000					
Al^{VI}	1.939	1.928					1.884
Ti	0.010	0.012		0.966		0.047	0.001
Cr	0.005	0.005		0.001		0.012	0.010
Fe^{3+}	0.041	0.040		0.066		1.861	0.104
Fe^{2+}	0.907	0.902		0.868		1.038	0.554
Mn	0.032	0.031		0.031			0.008
Mg	1.183	1.206		0.067		0.008	0.439
Ca	0.889	0.862					
Na							
total	8.005	7.997		1.999		3.000	3.000
Mg#	55.5	56.2					44.2
almandine	29.39	28.94	ilm	86.8	Fe_2TiO_4	4.6	0.1
andradite	2.06	2.02	geik	6.7	$FeCr_2O_4$	0.6	0.3
grossular	27.51	26.89	pyroph	3.1	hercynit	1.7	52.1
pyrope	39.71	40.82	hem	3.3	spinel	0.0	41.3
spessartine	1.07	1.06			magnetit	92.3	2.9
uvarovite	0.26	0.27			$MnAl_2O_4$	0.0	0.7
					$MgFe_2O_4$	0.7	2.3

Standard deviations 2σ (wt%) are as follows: 0.20 Si (Grt), 0.13 Al (Grt), 0.29, 0.70, 1.23 Fe (Grt, Ilm, Mt), 0.06 Mg (Grt), 0.17 Ca (Grt), 0.03, 0.46 Ti (Mt, Ilm), 0.09 Mn (Ilm).

Table 5. Trace element compositions of clinopyroxene and garnet from the eclogite BD112

Mineral	Clinopyroxene	Garnet (core)	Garnet (rim)
Li (ppm)	43	0.70	0.27
Rb	0.027	0.014	0.016
Sr	90	0.67	0.39
Y	3.7	81	62
Zr	72	48	47
Nb	0.13	0.022	0.015
Ba	0.38	0.036	0.026
La	4.65	0.099	0.095
Ce	18	1.5	1.1
Pr	3.5	0.67	0.48
Nd	18	6.5	5.4
Sm	4.0	3.5	3.8
Eu	0.95	1.4	1.6
Gd	2.3	5.6	5.7
Tb	0.25	1.4	1.2
Dy	1.1	12	10
Ho	0.15	3.0	2.4
Er	0.32	10	7.6
Tm	0.034	1.6	1.2
Yb	0.19	12	8.7
Lu	0.023	1.8	1.3
Hf	3.5	1.0	0.87
Ta	0.094	0.005	0.003
Pb	1.7	0.14	0.13
Th	1.4	0.13	0.14
U	0.54	0.42	0.35

For the precision and accuracy of the analyses, see Methods section

Always consult and cite the final, published document. See http://www.minsocam.org or GeoscienceWorld

Table 6. Composition of minerals in symplectite, sample BD110

mineral	anorthite	orthopyroxene	clinopyroxene	amphibole	spinel
analysis	20	1	19	3	15
SiO_2	42.99	51.04	50.51	46.75	
TiO_2		0.16	0.57	1.51	0.05
Al_2O_3	36.26	3.71	4.09	11.74	60.26
Cr_2O_3					0.49
FeO	0.41	18.43	6.88	10.07	29.64
MnO		0.82	0.33	0.22	0.35
MgO		23.72	14.07	14.55	11.11
CaO	19.92	0.57	23.45	12.79	
Na_2O				0.64	
total	99.58	98.45	99.90	98.27	101.9
oxygen No.	8	6	6	23	4
Si	1.997	1.903	1.879	6.604	
Al^{IV}	1.986	0.163	0.179	1.396	1.884
Al^{VI}				0.559	
Ti		0.004	0.016	0.160	0.001
Cr				0.000	0.010
Fe^{3+}	0.016	0.023	0.038	0.468	0.104
Fe^{2+}		0.552	0.176	0.721	0.554
Mn		0.026	0.010	0.026	0.008
Mg	0.003	1.318	0.780	3.064	0.439
Ca	0.991	0.023	0.934	1.936	
Na	0.007	0.000	0.006	0.175	
OH				2.000	
total	5.000	4.011	4.019	17.111	3.000

Always consult and cite the final, published document. See http://www.minsocam.org or GeoscienceWorld

This is a preprint, the final version is subject to change, of the American Mineralogist (MSA)
Cite as Authors (Year) Title. American Mineralogist, in press.
(DOI will not work until issue is live.) DOI: http://dx.doi.org/10.2138/am-2016-5298 7/15

Table 7. Composition of minerals in garnet peridotite BD134

	garnet			clinopyroxene		orthopyroxene		olivine
analysis	25	26		21	19	20	22	28
SiO_2	42.02	41.89		54.55	54.24	57.41	57.35	41.30
TiO_2	0.31	0.39		0.50	0.49	0.11	0.11	0.00
Al_2O_3	22.06	22.00		4.39	4.41	1.91	1.89	0.00
Cr_2O_3	1.65	1.62		1.01	1.05	0.28	0.24	0.02
FeO	8.45	9.35		2.49	2.69	6.37	6.55	9.98
MnO	0.31	0.35		0.06	0.07	0.14	0.19	0.17
MgO	20.50	19.71		15.03	15.35	33.76	33.65	48.23
CaO	4.66	4.63		20.36	19.87	0.42	0.36	0.04
Na_2O	0.04	0.04		2.22	2.25	0.02	0.01	0.02
total	99.99	99.97		100.62	100.41	100.42	100.36	99.74
oxygen No.	12	12		6	6	6	6	
Si	2.990	2.995		1.956	1.950	1.969	1.970	1.015
Al^{IV}	0.010	0.005		0.044	0.050			
Al^{VI}	1.844	1.851		0.141	0.137	0.077	0.077	
Ti	0.017	0.021		0.013	0.013	0.003	0.003	
Cr	0.093	0.091		0.029	0.030	0.008	0.007	
Fe^{3+}	0.041	0.033		0.001	0.014			
Fe^{2+}	0.462	0.526		0.074	0.067	0.183	0.188	0.205
Mn	0.019	0.021		0.002	0.002	0.004	0.006	0.004
Mg	2.174	2.101		0.803	0.822			1.766
Ca	0.355	0.355		0.782	0.765	1.726	1.723	0.001
Na				0.154	0.157	0.016	0.013	0.001
total	8.004	7.998		3.998	4.007	3.985	3.985	2.992
Alm	14.41	16.51	Acm	0.10	1.40			
Adr	2.08	1.66	Jd	14.20	13.68			
Grs	5.17	5.67	Ca-Ts	1.35	1.32	1.80	1.80	
Prp	73.03	70.81	En	40.20	41.10	86.30	86.13	
Sps	0.62	0.71	Fs	3.68	3.34	9.14	9.41	
Uv	4.69	4.62	Wo	37.60	36.41			
			CaCrAlPx	1.68	2.37	0.75	0.65	

Standard deviations 2σ (wt%) are as follows: 0.19–0.29 Si (Ol, Opx), 0.07–0.13 Al (Cpx, Grt), 0.12–0.23 Fe (Cpx, Ol), 0.11–0.19 Mg (Cpx, Ol), 0.07–0.22 Ca (Grt, Cpx).

Always consult and cite the final, published document. See http://www.minsocam.org or GeoscienceWorld

Fig. 1

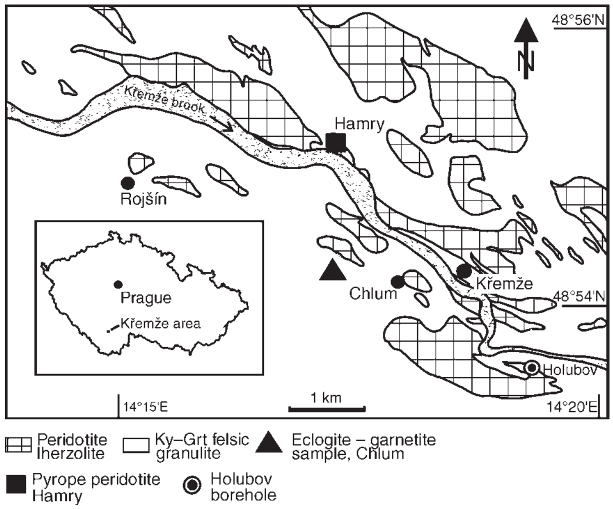
48°56'N
N
Křemže brook
Hamry
Rojšín
Prague
Křemže area
Chlum
Křemže
48°54'N
Holubov
14°15'E
1 km
14°20'E
Peridotite lherzolite
Ky–Grt felsic granulite
Eclogite – garnetite sample, Chlum
Pyrope peridotite Hamry
Holubov borehole

Fig. 2

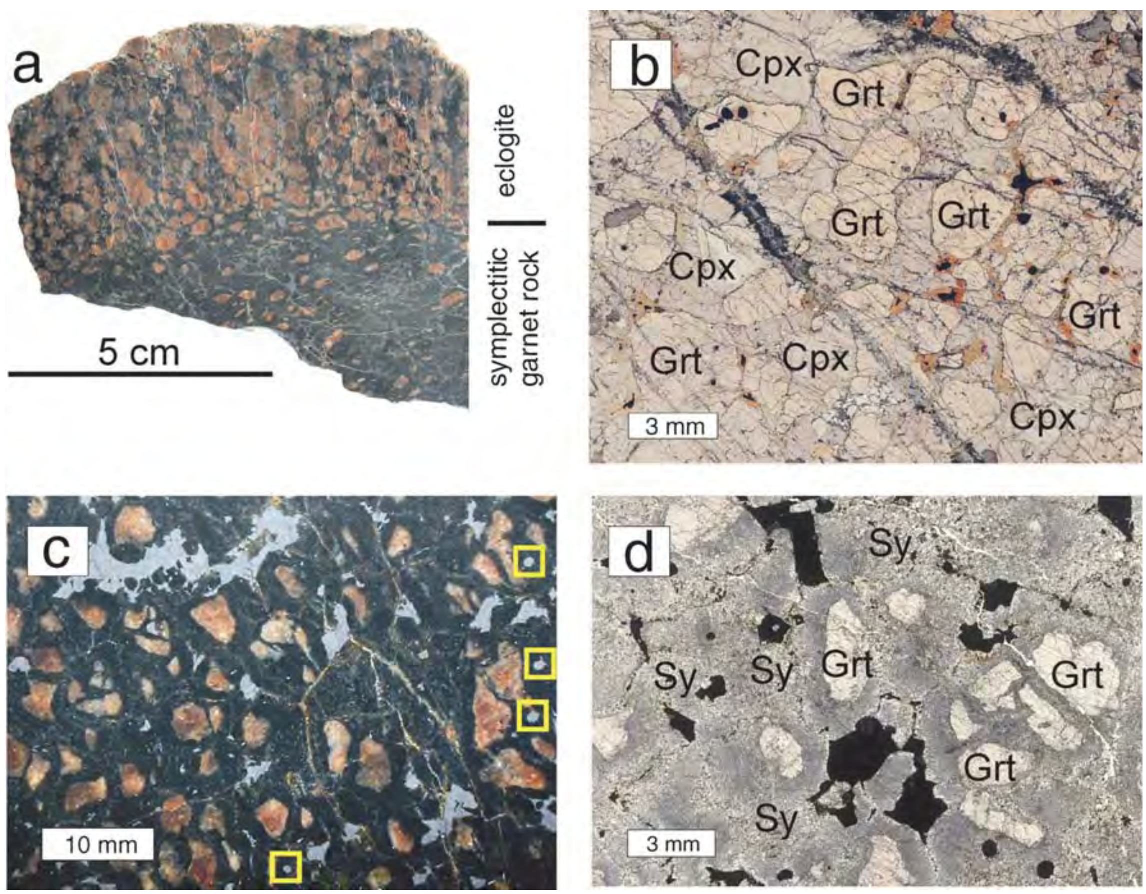
a
eclogite
symplectitic garnet rock
5 cm
b
Cpx
Grt
Grt
Grt
Cpx
Grt
Grt
Cpx
Cpx
3 mm
c
10 mm
d
Sy
Sy
Sy
Grt
Grt
Grt
Sy
3 mm

Fig. 3

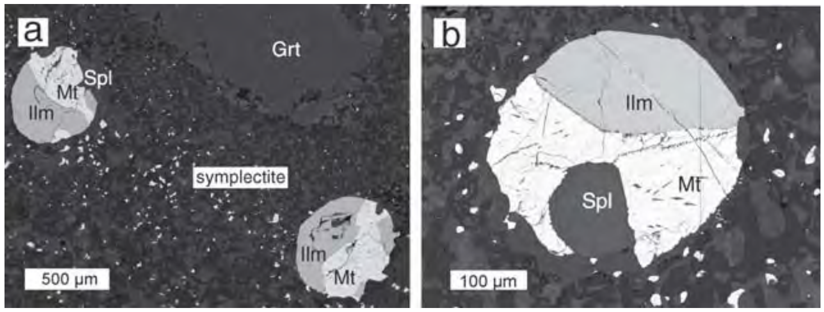

Fig. 4

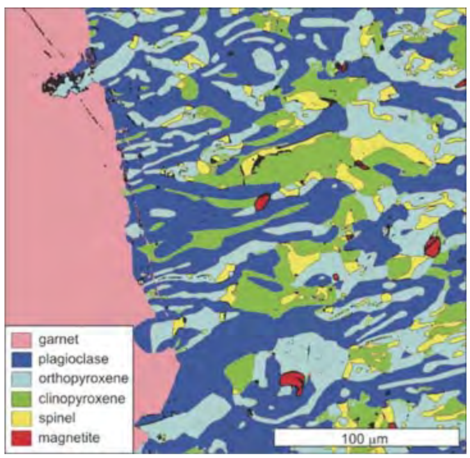

Fig. 5

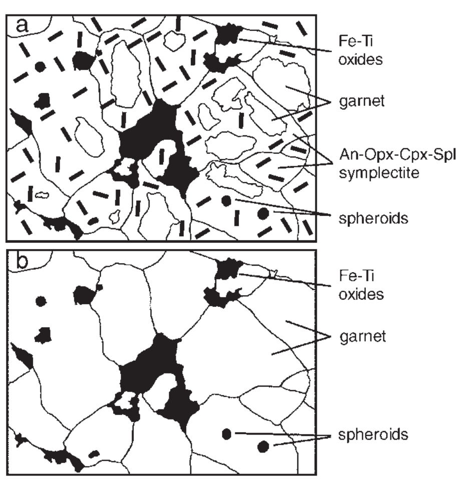

Fig. 6

Fig. 7

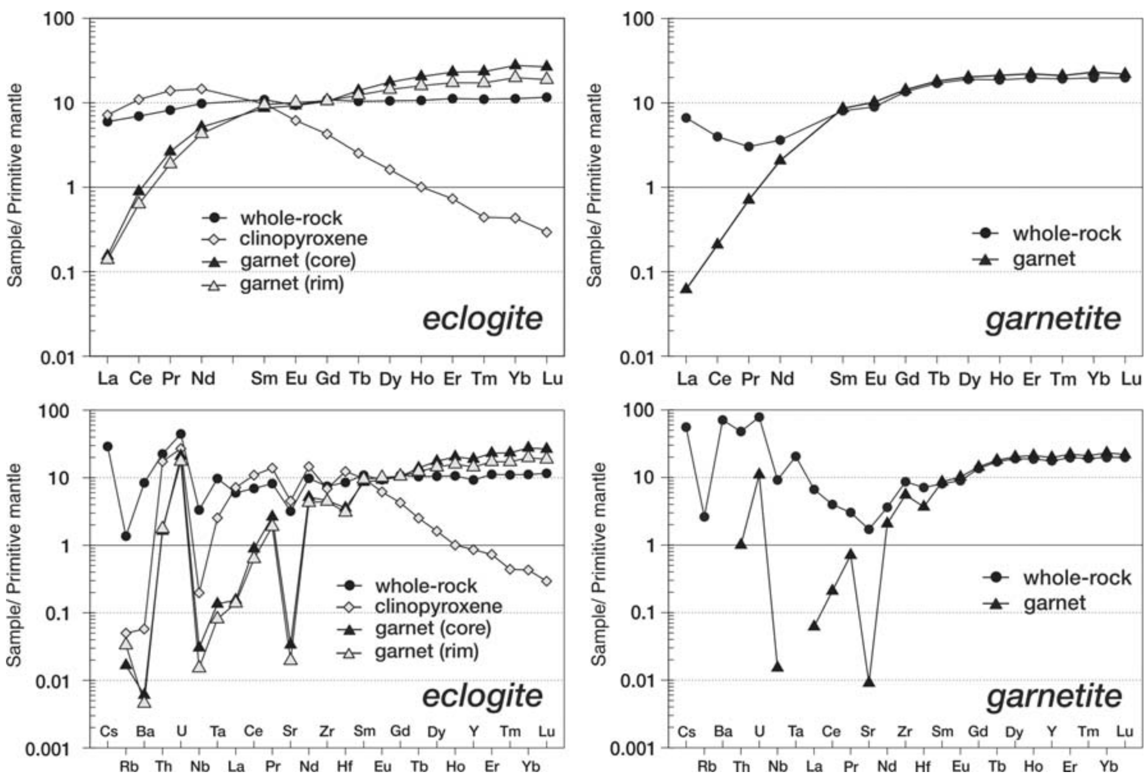

Always consult and cite the final, published document. See http://www.minsocam.org or GeoscienceWorld

Fig. 8

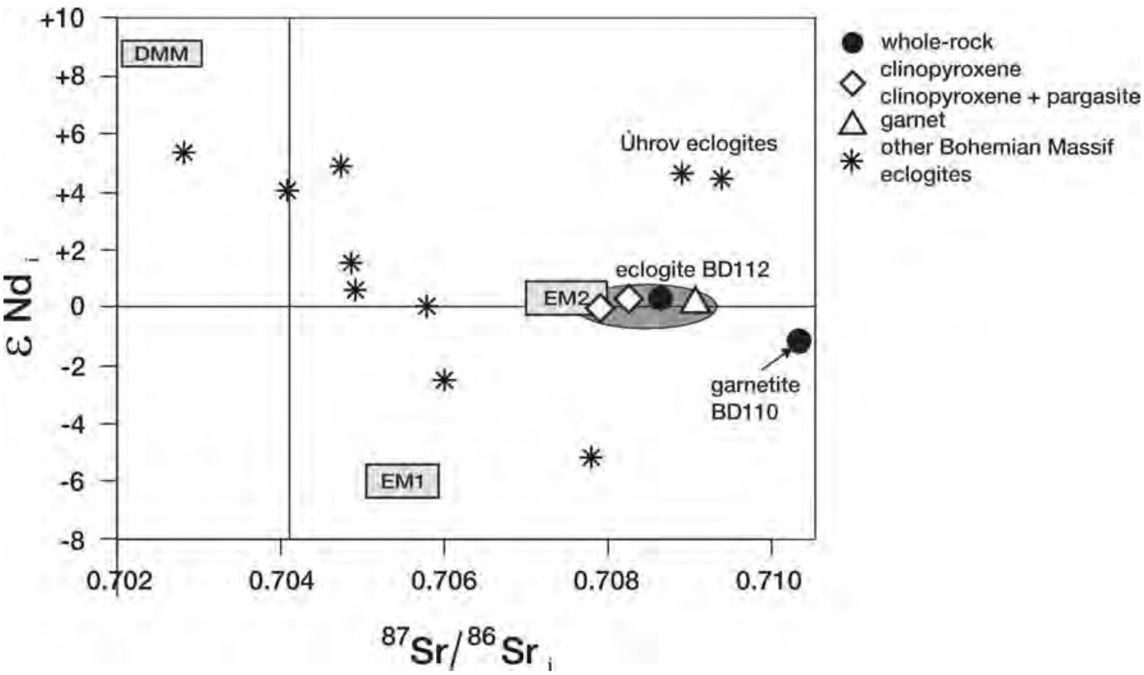

+10
+8
+6
+4
+2
0
-2
-4
-6
-8
DMM
EM2
EM1
ε Nd i
0.702
0.704
0.706
0.708
0.710
87Sr/86Sr i
Ůhrov eclogites
eclogite BD112
garnetite
BD110
whole-rock
clinopyroxene
clinopyroxene + pargasite
garnet
other Bohemian Massif
eclogites